Diffusion Modeling in a Generic Clay Repository

Fuel Cycle Research & Development

Prepared for
U.S. Department of Energy
Used Fuel Disposition
Liange Zheng, Hui-Hai Liu and Jens Birkholzer
Lawrence Berkeley National laboratory
W. Mark Nutt
Argonne National Laboratory

July 2011
FCRD-LBNL-2011-SLM

DISCLAIMER

This information was prepared as an account of work sponsored by an agency of the U.S. Government. Neither the U.S. Government nor any agency thereof, nor any of their employees, makes any warranty, expressed or implied, or assumes any legal liability or responsibility for the accuracy, completeness, or usefulness, of any information, apparatus, product, or process disclosed, or represents that its use would not infringe privately owned rights. References herein to any specific commercial product, process, or service by trade name, trade mark, manufacturer, or otherwise, does not necessarily constitute or imply its endorsement, recommendation, or favoring by the U.S. Government or any agency thereof. The views and opinions of authors expressed herein do not necessarily state or reflect those of the U.S. Government or any agency thereof.

FCT Quality Assurance Program Document

Appendix E
FCT Document Cover Sheet

Name/Title of Deliverable/Milestone: Diffusion Modeling in a Generic Clay Repository

Work Package Title and Number: Generic Disposal System-Level Modeling (FTLB11UF0325)

Work Package WBS Number: **1.02.08.03**

Responsible Work Package Manager: H.H. Liu (electronic signature)
(Name/Signature)

Date Submitted

Quality Rigor Level for Deliverable/Milestone	☐ QRL-3	☐ QRL-2	☐ QRL-1 ☐ Nuclear Data	☒ N/A*

This deliverable was prepared in accordance with Lawrence Berkeley National Laboratory
(Participant/National Laboratory Name)

QA program which meets the requirements of
☒ DOE Order 414.1 ☐ NQA-1-2000

This Deliverable was subjected to:

☐ Technical Review

Technical Review (TR)
Review Documentation Provided
☐ Signed TR Report or,
☐ Signed TR Concurrence Sheet or,
☐ Signature of TR Reviewer(s) below

Name and Signature of Reviewers

☐ Peer Review

Peer Review (PR)
Review Documentation Provided
☐ Signed PR Report or,
☐ Signed PR Concurrence Sheet or,
☐ Signature of PR Reviewer(s) below

*Note: In some cases there may be a milestone where an item is being fabricated, maintenance is being performed on a facility, or a document is being issued through a formal document control process where it specifically calls out a formal review of the document. In these cases, documentation (e.g., inspection report, maintenance request, work planning package documentation or the documented review of the issued document through the document control process) of the completion of the activity along with the Document Cover Sheet is sufficient to demonstrate achieving the milestone. QRL for such milestones may be also be marked N/A in the work package provided the work package clearly specifies the requirement to use the Document Cover Sheet and provide supporting documentation.

SUMMARY

Diffusion is the dominant mechanism for radionuclide transport in a clay repository. Modeling of diffusive transport in clay rocks is complicated by the existence of heterogeneity at different scales and coupling between diffusive and electro-chemical processes. This report reviews the two kinds of modeling approaches. Phenomenological approaches are based on Fick's diffusion law and use semi-empirical constants to roughly incorporate the effects of electro-chemical processes. While they cannot capture the detailed transport mechanisms and therefore inherently introduce a certain modeling uncertainty, they are relatively simple, computationally efficient, and straightforward to implement. Mechanistic approaches are based on detailed and explicit descriptions of interaction between diffusion processes and electro-chemical processes. They do not suffer the limitations of phenomenological approaches, but are computationally more complex and involve more parameters. This report also reviews and compiles data sets of parameters related to diffusive transport in clay formations that are available in the literature. These data sets provide useful information for evaluating modeling approaches and can be used as inputs into relevant models. An improved modeling approach is proposed to combine the advantages of phenomenological and mechanistic approaches. Results from a preliminary evaluation of the approach are encouraging. In the future, we will continue to evaluate the proposed modeling approach with more data, investigate the impact of heterogeneity on large-scale diffusion process, and integrate process modeling of diffusion in clay with system-level modeling.

CONTENTS

SUMMARY iv

1. INTRODUCTION 1

2. DIFFUSION THROUGH CLAY ROCK: A REVIEW 2
   2.1 Review of Modeling Approach 2
      2.1.1 Phenomenological Approach 2
      2.1.2 Mechanistic Approach 4
   2.2 Data For Transport Parameters of Clay Formations 6

3. AN IMPROVED MODELING APPROACH 15
   3.1 Theoretical Basis 15
   3.2 Preliminary Evaluation 17

4. CONCLUDING REMARKS 20

FIGURES

Figure 1. Clay/shale-formation distribution in the USA (Gonzales and Johnson 1984) 1

Figure 2. Measured and computed breakthrough curves of chloride with Single-Continuum Model (SCM) and Dual-Continuum Model (DCM) (Samper et al. 2008). 4

Figure 3. A diagram of the pore space in Opalinus Clay, showing three water types with associated diffusion domains (Appelo et al. 2010). 5

Figure 4. Comparison between calculated (curves) and observed (rectangles) values for ratio of diffusion coefficient as a function of charge number z_i. 18

Figure 5. Sketch of borehole geometry for DIR experiments (Samper et al. 2008) 19

Figure 6. Measured (Samper et al. 2008) and computed Cl concentration with several effective diffusion coefficients (m^2/s). 19

Figure 7. Measured (Samper et al. 2008) and computed Na concentration with several effective diffusion coefficients (m^2/s). 20

TABLES

Table 1. Estimated values for the effective diffusion coefficients D_e (m^2/s), effective diffusion coefficients in directions parallel and perpendicular to the clay-formation bedding, $D_{e\square}$ (m^2/s) and $D_{e\perp}$ (m^2/s), accessible porosity ε, distribution coefficient K_d (mL/g), apparent diffusion coefficient D_a (m^2/s), apparent diffusion coefficients in directions parallel and perpendicular to the bedding, $D_{a\square}$ (m^2/s) and $D_{a\perp}$ (m^2/s), retardation coefficient R, rock capacity factor α, and the factor in directions parallel and perpendicular to the bedding of other clay formations, $\alpha_\square$ and $\alpha_\perp$ 10

Table 2. The minimum, maximum and average values for the effective diffusion coefficient D_e (m^2/s), accessible porosity ε, distribution coefficient K_d (mL/g), rock capacity factor α for Opalinus Clay. 12

Table 3. Estimated data for the effective diffusion coefficients D_e (m^2/s), effective diffusion coefficients in directions parallel and perpendicular to the bedding of clay formation , $D_{e\square}$ (m^2/s) and $D_{e\perp}$ (m^2/s), accessible porosity ε, distribution coefficient K_d (mL/g), apparent diffusion coefficients in directions parallel to the bedding, $D_{a\perp}$ (m^2/s), and rock capacity factor α for Callovo-Oxfordian (COx) argillite. 12

Table 4. The minimum, maximum and average values for effective diffusion coefficient D_e (m^2/s), accessible porosity ε, distribution coefficient K_d (ml/g) for COx argillite. 13

Table 5. Estimated values for effective diffusion coefficients D_e (m^2/s), accessible porosity ε, and distribution coefficient K_d (mL/g) for Toarcian clayey formation at the Tournemire experimental site (France). 13

Table 6. The minimum, maximum and average values for the effective diffusion coefficient D_e (m^2/s), accessible porosity ε, distribution coefficient K_d (mL/g) for Toarcian clayey formation at the Tournemire experimental site (France). 15

Table 7. Values for effective diffusion coefficient (m^2/s) of different species for Opalinus Clay (OPc), Callovo-Oxfordian (COx) argillite and Toarcian clayey formations (TOc) 15

Table 8. Values for accessible porosity of different species for Opalinus Clay (OPc), Callovo-Oxfordian (COx) argillite, and Toarcian clayey formations (TOc) 15

ACRONYMS

COx, Callovo-Oxfordian

DCM, Dual-Continuum Model

DDL, Diffusive Double Layer

EBS, Engineered Barrier System

EDZ, Excavation Disturbed Zone

FEP, Features, Events and Processes

HLW, High-Level Waste

HTO, Tritiated Water

IRSN, Institute of Radiopretection and Nuclear Safety

OPA, Opalinus Clay

REV, Representative Elementary Volume

SCM, Single-Continuum Model

DIFFUSION MODELING IN A GENERIC CLAY REPOSITORY

1. INTRODUCTION

Clay/shale has been considered as potential host rock for geological disposal of high-level radioactive waste throughout the world, because of its low permeability, low diffusion coefficient, high retention capacity for radionuclides, and capability to self-seal fractures. For example, Callovo-Oxfordian argillites at the Bure site, France (Fouche et al. 2004), Toarcian argillites at the Tournemire site, France (Patriarche et al., 2004a), Opalinus Clay at the Mont Terri site, Switzerland (Meier et al. 2000), and Boom clay at the Mol site, Belgium (Barnichon and Volckaert 2003) have all been under intensive scientific investigation (at both field and laboratory scales) for understanding a variety of rock properties and their relationships to flow and transport processes associated with geological disposal of radioactive waste. Figure 1 presents the distribution of clay/shale formations within the USA.

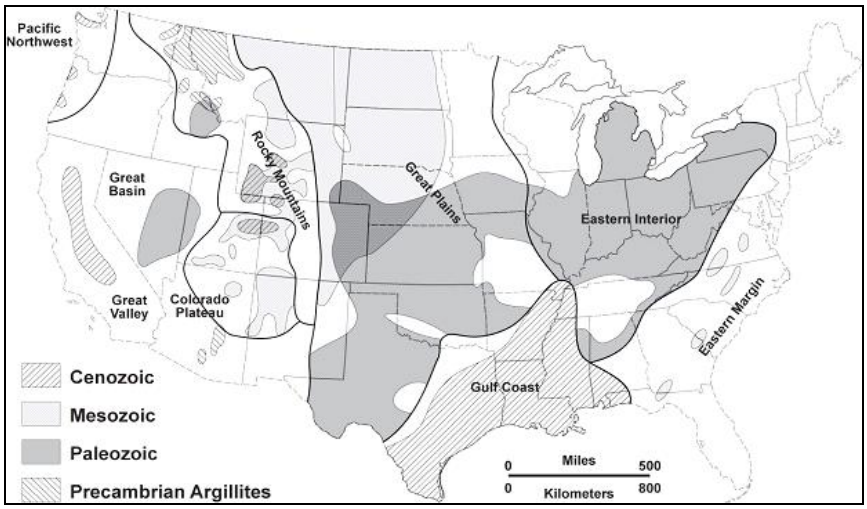

Figure 1. Clay/shale-formation distribution in the USA (Gonzales and Johnson 1984)

Owing to the low permeability of clay rock, diffusion may be the dominant mechanism for radionuclide transport in a clay formation. Exceptions possibly include areas where flow velocities may be larger, e.g., within the excavation disturbed zone (EDZ) where highly-permeable fractures are induced by tunnel excavation or along natural features such as faults or intrusions disrupting the formation. The overall objectives of this work activity are to summarize the state of the art for modeling diffusion process in natural clay formations, to review analysis results from diffusion experiments on clay rock that are available in the literature, to evaluate the impact of relevant processes on diffusion, and to develop simplified diffusion process models that can be used to support the development of the system-level diffusion model for natural clay formations. This work activity addresses Features, Events and Processes FEP 2.2.09, Chemical Process—Transport (shale), which has been ranked medium in importance, as listed in Table 7 of the *Used Fuel Disposition Campaign Disposal Research and Development Roadmap* (FCR&D-USED-2011-000065 REV0) (Nutt 2011).

This report documents progress that has been made in FY11, including a review of the modeling approach and parameter data sets (Section 2), as well as a preliminary evaluation of a newly proposed modeling approach (Section 3). The summary and a discussion of future work are given in Section 4.

2. DIFFUSION THROUGH CLAY ROCK: A REVIEW

This section presents a review of approaches to modeling diffusion processes in natural clay formations, and parameter data obtained from relevant experimental observations.

2.1 Review of Modeling Approach

Modeling of diffusive transport in clay rocks (natural system) is complicated by the existence of heterogeneity at different scales and coupling between diffusive and electrochemical processes (Revil and Leroy 2004; Appelo et al. 2010; Bourg et al. 2003; Jougnot et al. 2009). At a local scale, different pore spaces co-exist within a representative elementary volume (REV), or a "point" within the context of continuum mechanics. They include pore spaces surrounded by grains other than clay, pore spaces surrounded by clay and other grains, pore spaces surrounded by clay grains only, and interlayer spaces within clay grains. The dominant transport processes of radionuclides can be quite different for these different kinds of pore spaces. For example, the coupling between diffusive and electrochemical processes, or the interaction between diffusion in bulk fluid and an electrical double-diffusion layer near clay surfaces, is negligible for pores surrounded by other grain particles, but critical for small pores surrounded by clay particles and interlayer spaces. The last two pore-space types are especially important for compacted clay systems (such as clay buffers in Engineered Barrier System (EBS)) and also highly relevant for natural clay rock. Modeling approaches for diffusion differ in their treatment of these different types of pores and in their considerations of the electrochemical processes. In the literature, specifically two kinds of modeling approaches are available for describing diffusive transport in clay materials (Bourg et al. 2003; Revil and Leroy 2004; Appelo et al. 2008; Jougnot et al. 2009; Appelo et al. 2010): the phenomenological approach and the mechanistic approach.

2.1.1 Phenomenological Approach

The phenomenological approach, a modeling approach based on Fick's diffusion law, uses semi-empirical constants to roughly incorporate the effects of electrochemical processes, such as using the "accessible porosity" to consider anion exclusion effects. While this kind of approach cannot capture detailed transport mechanisms, it is relatively simple, computationally efficient, and straightforward to implement.

Typically, using this approach, the diffusive transport equation is given as:

$$\epsilon R \frac{\partial C}{\partial t} = \nabla \cdot (D_e \nabla C) \tag{1}$$

where C is concentration, t is the time, ϵ is porosity, D_e is effective diffusion coefficient and R is retardation factor which is given by the following equation:

$$R = 1 + \frac{\rho K_d}{\epsilon} \tag{2}$$

where ρ is the dry density of the solid and K_d is the distribution coefficient.

The effective diffusion coefficient is treated as an empirical parameter and is related to the diffusion coefficient of a chemical species in free water by the following equation (e.g., Appelo and Wersin 2007; Appelo et al. 2010):

$$D_e = \epsilon D_p = \epsilon \frac{\delta}{\theta^2} D_w \tag{3}$$

where D_p is the pore-water diffusion coefficient, D_w is the diffusion coefficient in free water, θ^2 is the tortuosity factor, which accounts for the fact that diffusing molecules must pass around solid grains and take a longer path than a straight-line distance, and δ is the constrictivity factor, encompassing the effect of pore narrowing and widening (Appelo et al. 2010). Because it is difficult to derive θ^2 and δ theoretically, researchers tend to obtain them (or a geometrical factor *G* ($\frac{1}{G} = \frac{\delta}{\theta^2}$) that combines them) by fitting laboratory or field test data. Some researchers do not even bother to calibrate them — they calibrate effective diffusion coefficient directly.

In many cases, Equation (3) has been observed to underpredict the diffusion of cations (e.g., Bourg et al. 2003). This is often interpreted as resulting from the diffusion of adsorbed species along the solid surface. Therefore, as reviewed by Bourg et al. (2003), a semi-empirical effective "surface diffusion coefficient" was introduced to take this effect into account:

$$D_{e,surf} = \frac{D_{surf} \rho K_d}{\theta^2} \tag{4}$$

where D_{surf} is the so-called surface diffusion coefficient, and subscript *e* refers to effective parameters throughout this report. The derivation of Equation (4) was based on an assumption that tortuosity factors are the same for pore space and surface paths (Bourg et al. 2003). Note that the summation of effective diffusion coefficients given in Equations (3) and (4) should be used in Equation (1) for cations.

Negative adsorption of anions — electrostatic anion exclusion from the diffuse layer due to the negative charge of the solid — calls for a further adjustment through replacing a geometrical porosity in Equation (1) by a so-called accessible porosity. The latter is generally smaller than the former, to account for the fact that within clay, as a result of anion exclusion, a fraction of the porosity does not participate in anion diffusion.

The phenomenological approach has occasionally been extended by considering different types of pores (pore spaces surrounded by clay versus those surrounded by other grains), resulting in a type of model that is usually referred to as a *dual-continuum* or *dual-porosity* model (Samper et al. 2008; Zheng and Samper 2011). The dual-continuum model is motivated by limitations in the phenomenological approach based on a single continuum: this approach has failed to interpret some laboratory or field diffusion test results. For example, Figure 2 shows the breakthrough curve of chloride for a permeation test using FEBEX bentonite (Samper et al. 2008). Similar behavior was also observed for the diffusion of tritiated water (HTO) in a natural clay sample (Opalinus Clay) (van Loon and Jakob 2005). Samper et al. (2008) showed that the single-continuum model with optimal effective diffusion coefficient and accessible porosity, calibrated by an inverse methodology, fails to reproduce the measured long tail of the breakthrough curve of chloride—whereas the dual-continuum model does a better job, as shown in Figure 2. The dual-continuum model was first developed for matrix-fracture systems (Barenblatt and Zheltov

1960; Pruess and Narasimhan 1985) and later applied to structured natural soil (Gerke and van Genuchten 1993a; 1993b; Gerke and van Genuchten 1996; Ray et al. 1997; Hantush et al. 2000 ; Lichtner 2000; Hantush et al. 2002; Šimunek et al. 2003). When applying such a model to a clay formation or compacted bentonite, the concept is to divide the porous media system into two continua: one associated with the pores surrounded by clay particles, and the other tied with those surrounded by other grains. The division is either arbitrary (Wilson et al. 1992) or based loosely on the physical characteristics of the soil (Ray et al. 1997). Equation (1) is applied to both continua, and the mass transfer between the two continua are either calculated by solving the mass-transfer equation perpendicular to the flow direction in the continua (Lichtner 2000) or by a lumped transfer term with a first-order (Gerke and van Genuchten 1993a; 1993b) or higher-order form (Zheng and Samper 2011).

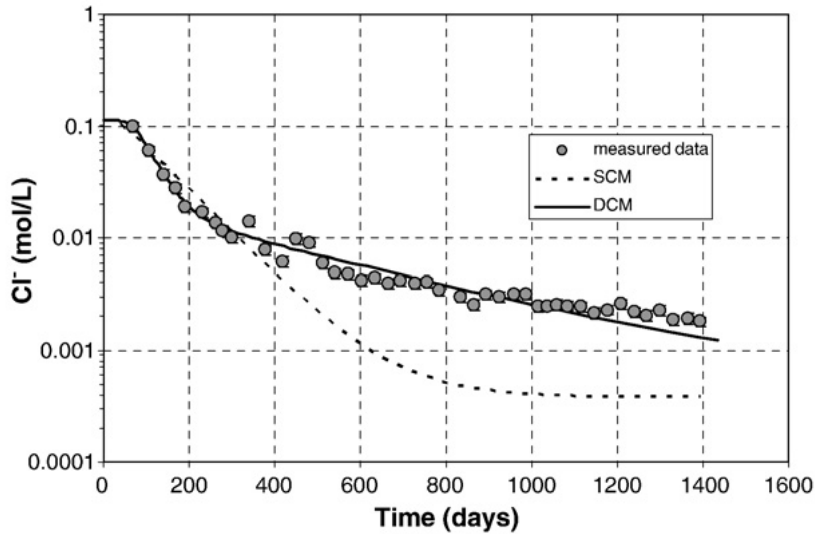

Figure 2. Measured and computed breakthrough curves of chloride with Single-Continuum Model (SCM) and Dual-Continuum Model (DCM) (Samper et al. 2008).

In summary, the phenomenological approach is largely based on a conventional approach to model contaminant transport in porous media, one that essentially ignores the effects of details of electrochemical processes. As a result of its computational and conceptual simplicity, this approach seems to be a natural choice for system-level modeling studies. However, some uncertainties exist when applying it to natural clay formations. As reviewed below in Section 2.2, although reasonable success with this approach has been achieved with calibrated effective parameters, most experiments (including field tests) used to evaluate this approach were conducted at relatively small scales. It remains to be determined if extrapolation of results from small scales to large scales relevant to a clay geological formation will provide results representative of the actual process. This is simply because our knowledge of how electrochemical processes affect large-scale diffusion is still lacking at this point. Furthermore, most of the effective parameters using this approach are not rigorously defined. Care must be taken when applying the measured values for these parameters to problems in which the corresponding conditions are different. For example, accessible porosity is used to account for the impact of anion exclusion. The latter, however, would likely vary with ionic strength and the charge of the anion in question, and therefore cannot be predicted using an adjusted accessible porosity. In other words, estimated values for accessible porosity are not constants, but a function of experimental conditions.

2.1.2 Mechanistic Approach

Mechanistic approaches are based on detailed and explicit descriptions of interactions between diffusion processes and electrochemical processes. Development of improved mechanistic approaches for diffusion processes in clay buffers (bentonite) is an active research activity in the EBS work package. A review of mechanistic approaches within the context of diffusion in bentonite was already provided by Steefel et al. (2010). As a result, we give only a very brief discussion of mechanistic approaches here. However, it is important to note that our interest here is mainly in diffusion within natural clay rock. Although the mechanistic approaches developed for bentonite, in principle, can be applied to natural clay rock, there are some notable differences between features of natural clay rock and bentonite that are relevant to diffusion processes. For example, unlike the EBS bentonite, which contains large proportions of clay minerals (e.g. FEBEX bentonite has 92% of smectite (ENRESA 2000)), clay rock has a relatively small percentage of smectite clay minerals. For example, Opalinus Clay has only 10% of an illite/smectite mixture (Thury 2002). The pore space surrounded by the clay minerals therefore only accounts for a relatively small portion of whole pore space.

One important feature of clay is that a clay particle's surface is negatively charged, which creates a so-called diffuse double layer (DDL). Figure 3 presents a schematic diagram of pore space in Opalinus Clay (Appelo et al. 2010). In a typical pore surrounded by clay, the pore water (close to the surface of the clay) becomes charged by an excess of anions and a deficit of cations, and turns into a DDL. Mechanistic approaches tend to explicitly consider the coupling between diffusive and electrochemical processes, i.e., the diffusion through the free solution and the interaction with DDL (Appelo et al. 2008; Jougnot et al. 2009; Appelo et al. 2010). For example, Appelo et al. (2010) divide water in pore space into three parts, based on their different physical and chemical properties: mobile pore water (that is not impacted by electrochemical processes), DDL water near the pore walls, and interlayer water (occupying spaces between clay layers). Then, the diffusion processes in the three parts and their interactions (or couplings) are modeled.

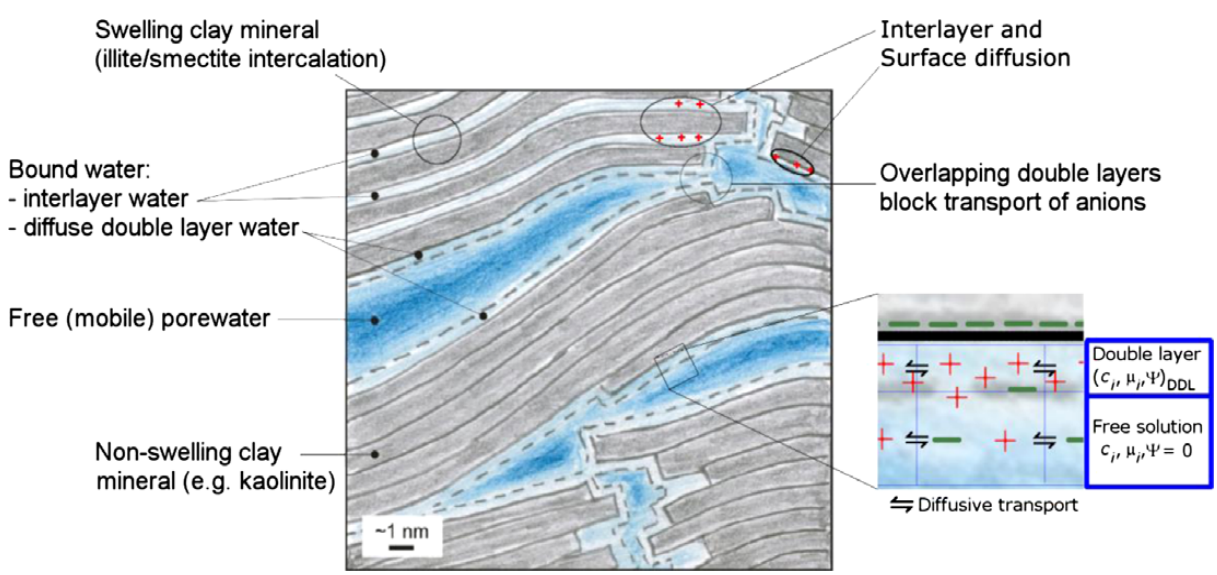

Figure 3. A diagram of the pore space in Opalinus Clay, showing three water types with associated diffusion domains (Appelo et al. 2010).

While a number of mechanistic approaches are available, they are all generally much more complicated than the phenomenological approach and have the following three common features. First, the diffusive flux of a species is the result of both a chemical and electrical potential gradient (Appelo and Wersin 2007). In the other words, the commonly used Fick's law is in general not considered to be applicable

anymore. Second, DDL is explicitly incorporated, and the concentrations in DDL are linked to the concentrations in free solution by Boltzmann's equation or Donnan approximation (Appelo and Wersin 2007). Third, the adsorption of ions is calculated by combining a surface complexation model and the DDL (Appelo et al. 2010).

In general, since the electrochemical processes are relatively rigorously considered in a mechanistic approach, this approach does not have the limitations of a phenomenological approach, mentioned in Section 2.1.1. However, this kind of approach is computationally more complex, involves more parameters, and therefore needs more experimental data to identify parameter values. It may be of interest to indicate that the related parameter values are spatially variable in a natural clay formation, because of the existence of heterogeneity at different scales, which likely increases the burden for parameter determination. This issue, however, may not be a problem for EBS bentonite because, at the continuum scale, heterogeneity for bentonite is minor, as a result of the way it is packed.

2.2 Data For Transport Parameters of Clay Formations

This section documents parameter data sets related to diffusion processes in clay formations that are available in the literature**.** In this section, by "measured" parameters, we mean those estimated based on the phenomenological approach (discussed in Section 2.1.1) from diffusion experiments. Also, while our compilation of the data sets includes typical ones for clay formations, it by no means is exhaustive.

Opalinus Clay (OPA) is a geological formation in the northern part of Switzerland with suitable properties for hosting a repository for high-level radioactive waste (Thury 2002). Table 1 summarizes the measured OPA property values, including effective diffusion coefficients D_e, effective diffusion coefficients in directions parallel and perpendicular to the bedding of clay formation , $D_{e\square}$ and $D_{e\perp}$, accessible porosity ε, distribution coefficient K_d, apparent diffusion coefficient D_a, apparent diffusion coefficients in the directions of parallel and perpendicular to the bedding, $D_{a\square}$ and $D_{a\perp}$, retardation coefficient R, rock capacity factor α and rock capacity factor for directions parallel and perpendicular to the bedding , $\alpha_{\square}$ and $\alpha_{\perp}$. As for the entities listed in Table 1, they are related through the following equations:

$$D_a = \frac{D_e}{\alpha} \tag{5}$$

$$\alpha = \epsilon R \tag{6}$$

Apparently, for non-adsorbed species, Equation (6) becomes:

$$\alpha = \epsilon \tag{7}$$

In Table 1, the values directly reported in the corresponding references are shown in the cell with white background, and those with yellow background are derived according to Equation (5) to (7). To make the inter-reference comparison, two difficulties need to be overcome. First, different researchers chose different type of parameters to report. For example, Cormenzana et al. (2008) reported the accessible porosity and apparent diffusion coefficients for HTO, whereas Van Loon et al. (2004a) reported the rock capacity factor and effective diffusion coefficients for HTO. Second, diffusion processes through the OPA exhibit anisotropy, with a diffusion coefficient parallel to clay-formation bedding that is higher than that perpendicular to the bedding. When conditions allowed—for example, as three dimensional laboratory or *in situ* data became available for model calibrations—values for diffusion coefficient and

rock capacity factor in both directions ($D_{e\square}$ and $D_{e\perp}$) were reported (Van Loon et al. 2004a; Garcia-Gutierrez et al. 2006; Samper et al. 2008). On the contrary, most in- or through-diffusion tests do not allow for calibration of the anisotropic diffusion coefficients (Van Loon et al. 2003; Van Loon et al. 2003; Maes et al. 2008; Wersin et al. 2008; Wu et al. 2009), and single values for the diffusion coefficient (D_e) were reported.

We therefore make the following adjustment to make different sets of data comparable. First, we use the effective diffusion coefficient, accessible porosity, and rock capacity factors as the parameters to be compared. For example, if apparent diffusion coefficients are reported (D_a), they are converted to an effective diffusion coefficient (D_e). Second, we take $D_e = \frac{D_{e\parallel} + D_{e\perp}}{2}$ to overcome the difficulty when anisotropic effective-diffusion coefficients are reported in one reference while non-anisotropic ones are reported in other references. Table 2 presents values for the maximum, minimum, and average for effective diffusion coefficient, accessible porosity, and rock capacity factor. The diffusion coefficient of HTO has been measured quite extensively. The accessible porosity for HTO is usually close to the physical porosity of OPA and represents the upper bound of diffusive porosity for other species. The difference between minimum and maximum diffusion coefficient of HTO is about one order of magnitude. Accessible porosity for HTO ranges from 0.1 to 0.16, with most values reported around 0.15 (see Table 1). Only the effective diffusion coefficient and accessible porosity of D_2O (deuterium) are reported in Samper et al. (2006), which are calibrated from a 3D model based on the DI-B *in situ* test for OPA. They are quite close to those values for HTO. It is known that chloride is subject to anion exclusion and has an accessible porosity smaller than that for a neutral species such as HTO. As shown in Table 2, the accessible porosity for chloride ranges from 0.039 to 0.081, with an average of 0.059, which is about 40% of the porosity for HTO. Because of the smaller accessible porosity, the effective diffusion coefficient for chloride is also smaller, about 13% of that for HTO. The measured effective diffusion coefficient for chloride varies significantly, with a difference between minimum and maximum values that is more than one order of magnitude.

Iodide has slightly higher accessible porosity than chloride, probably because iodide is weakly adsorbed (Savoye et al. 2006a). The average effective diffusion coefficient for iodide is also slightly higher than that for chloride. Only diffusion coefficient and accessible porosity for bromide are reported in Van der Kamp and Van Stempvoort (1998), cited in Van loon et al. (2004b), and both are much higher than those for chloride and iodide, which leads to questioning the reliability of the data. For cations, Table 2 lists values for the rock capacity factor instead of accessible porosity, because cations are usually adsorbed. The measured effective diffusion coefficient for sodium is quite consistent with the ratio of the maximum to the minimum (2.5), based on the four data points from Van Loon et al. (2004a; 2004b). The average effective diffusion coefficient is about 1.6 fold that of HTO. Sodium is not very strongly adsorbed. Its rock capacity factor ranges from 0.55 to 1 and the average is 0.7. Cesium, on the other hand, is very strongly adsorbed and has an average rock capacity factor of 3570. The large rock capacity factor for cesium leads to a large effective diffusion coefficient, which is about 20 times higher than that for HTO. Diffusion coefficient and rock capacity data for neptunium (V) was only reported in Wu et al. (2009). The rock capacity factor is lower than that for cesium, but the measured effective diffusion coefficient is much smaller than that for HTO. Note that for highly adsorbed cations, measured concentration or flux data are not very sensitive to the diffusion coefficient, so that the calibrated diffusion coefficient might have rather large uncertainty.

The Callovo-Oxfordian (COx) argillite formation is a candidate host rock for disposal of high-level radioactive waste in France. Although diffusion through the COx argillite was not as widely studied as the diffusion through the OPA, several researchers have reported values for related parameters such as diffusion coefficient, accessible porosity, and distribution coefficient for COx argillite. Reported

parameters are summarized in Table 3. The entities derived from originally reported ones are in the cells with yellow background, while others are directly taken from the literature. In Table 3, reported values for rock capacity factor (called apparent porosity by the authors in the literature) (Descostes et al. 2008) for HTO, chloride, iodide, SeO_3^{-2}, and SO_4^{-2} are taken to be the same as accessible porosity, with the assumption that these neutral and anionic species are not adsorbed. When effective diffusion coefficients in directions parallel and perpendicular to the bedding of clay formation, $D_{e\square}$ and $D_{e\perp}$, are reported, the averages of these coefficients are taken when comparing with the D_e (not considering anisotropic diffusion coefficients) reported by others.

Based on the data listed in Table 3, we calculated the minimum, maximum, and average for effective diffusion coefficient D_e, accessible porosity ε, and distribution coefficient K_d for COx argellite (Table 4). The effective diffusion coefficients of HTO for COx are quite consistent from different sources, ranging from 1.1e-11 to 4.9e-11 m^2/s, with an average of 3.1e-11 m^2/s. The accessible porosities of HTO for COx, however, show rather large variations, with a range from 0.15 to 0.25, partially because of some large values reported in Descostes et al. (2008). Descostes et al. (2008) measured the porosity of COx argillite samples taken from different depths of a core. The compositional difference (for example, between the content of clay) might be the possible reason for such variations in porosity. Note that the porosity value reported by Garcia-Gutierrez et al. (2008) (see Table 3) is obtained by the measurement of dry density and grain density. The steady-state concentration profiles collected in Garcia-Gutierrez et al. (2008) from through-diffusion and in-diffusion do not allow for calibration of porosity. The effective diffusion coefficient of chloride for COx seems to exhibit large variation, with a minimum value of 4.8e-13 m^2/s and a maximum value that is about 20 times the minimum one. However, if we leave out 4.8e-13 m^2/s from Descostes et al. (2008), the rest are quite consistent, ranging from 4.4e-12 to 9.1e-12 m^2/s (The reliability of the measured value of 4.8e-13 m^2/s needs to be further examined). The accessible porosity of chloride ranges from 0.05 to 0.09, with an average of 0.07. The effective diffusion coefficients of iodide show small variation, whereas the accessible porosity does not. Again, we call attention to the abnormally large ε value of 0.284 from Descostes et al. (2008). Also reported in Descostes et al. (2008) are the diffusion coefficients and accessible porosities for SeO_3^{-2} and SO_4^{-2}. Some notable observations from these data are: (1) the low effective diffusion coefficient, especially for SeO_3^{-2}, which seems to suggest that the bivalent anions have a lower diffusion coefficient than monovalent ones; and (2) the low accessible porosity for SeO_3^{-2} (about one order of magnitude smaller than that for chloride), which seems to suggest that bivalent anions suffer a more significant anion exclusion effect than monovalent, although the accessible porosity for SO_4^{-2} does not show this behavior. It should be noticed that iodide and SO_4^{-2} are weakly adsorbed—the accessible porosity values listed in Table 4 really are those for rock capacity factor, a product of accessible porosity and retardation factor—which explains why those values are higher. Parameters for three cations—sodium, strontium and cesium—have been reported. Their accessible porosities are similar to that for HTO, all of them are adsorbed, and their diffusion coefficients are not always larger than that for HTO. The values for the effective diffusion coefficients of sodium and cesium are larger than that for HTO, whereas that for strontium is lower.

Diffusion parameters for the Toarcian clayey formation at the Tournemire experimental site (France) have been studied by several researchers (Patriarche et al. 2004b; Savoye et al. 2006b; Motellier et al. 2007). The Tournemire site is a French experimental site chosen by the Institute for Radioprotection and Nuclear Safety (IRSN) to evaluate the migration processes of chemical species through an argillaceous formation (argillites), similar to those studied elsewhere for radioactive waste disposal. Table 5 lists the measured effective diffusion coefficients D_e, accessible porosity ε, and distribution coefficient K_d, for the Toarcian clayey formation, while Table 6 summarizes the minimum, maximum, and average values for the effective diffusion coefficient D_e, accessible porosity ε, distribution coefficient K_d. Motellier et al. (2007) measured the effective diffusion coefficients of HTO for several samples under different

conditions: with and without fractures or in different orientations. Measured data are quite consistent except for two smaller values: 7.5e-12 and 7.9e-12, which are measured from an orientation 90° to the horizontal direction (not necessarily perpendicular to the clay-formation bedding). As for parameters listed in Table 6 for chloride, iodide, and bromide, note the large variation in the accessible porosity for iodide and the weak adsorption of iodide.

As a result of subsurface heterogeneity, diffusion properties vary for a given species within the same clay formation. Effective diffusion coefficient, accessible porosity, and distribution coefficient for the same chemical species also change according to the type of clay formation. So far, we have compiled data for three types of clay formation: Opalinus Clay (OPA), Callovo-Oxfordian (COx) argillite, and Toarcian clayey. Table 7 shows variations in the effective diffusion coefficient among these formations. The large ratios of the maximum value to the minimum value show the significant variability in effective diffusion coefficient. The ratio for HTO associated with OPA is about 10. For the rest of the species, the largest ratio is 22 for iodide associated with OPA, and smallest one is 2.4 for sodium associated with COx. Unlike the diffusion coefficient calibrated from the measured concentration (or flux) data from a diffusion test, the accessible porosity for HTO, usually assumed to be the total porosity, can be measured directly (e.g., by measuring nitrogen or mercury adsorption) or indirectly (e.g., by measuring the dry density and grain density). Therefore, the accessible porosity for HTO has relatively small variation (Table 8). However, the accessible porosity of chloride and iodide (that is subject to anion exclusion) must be calibrated and therefore has the larger porosity ratio of the maximum to minimum values, up to 7 for iodide (Table 8). Note that iodide can also be adsorbed.

There are several reasons for the variations in measured diffusion parameters within a given species and clay formation. First, the consistency between results from different types of laboratory and field diffusion tests (such as percolation experiments, pulse injections, through-diffusion and in-diffusion tests) is a concern (Aertsens et al. 2008). Second, the spatial heterogeneity of a clay formation is an important source of variation in parameters. Samples taken from different locations or tests conducted at different places can lead to quite different results. For example, *in situ* tests DI-A2 (Wersin et al. 2008) and DI-A1 (Van Loon et al. 2004a) have the same setup but are located 1 m apart. The diffusion coefficients for HTO, I- and Cs+ are quite different for these two tests. Third, the anisotropy of a given clay sample apparently can cause variation in parameters along different directions (e.g., Cormenzana et a. 2008; Van Loon et al. 2004a;, Motellier et al. 2007).

Table 1. Estimated values for the effective diffusion coefficients D_e (m^2/s), effective diffusion coefficients in directions parallel and perpendicular to the clay-formation bedding, $D_{e\square}$ (m^2/s) and $D_{e\perp}$ (m^2/s), accessible porosity ε, distribution coefficient K_d (mL/g), apparent diffusion coefficient D_a (m^2/s), apparent diffusion coefficients in directions parallel and perpendicular to the bedding, $D_{a\square}$ (m^2/s) and $D_{a\perp}$ (m^2/s), retardation coefficient R, rock capacity factor α, and the factor in directions parallel and perpendicular to the bedding of other clay formations, $\alpha_\square$ and $\alpha_\perp$.

Species	D_e	$D_{e\square}$	$D_{e\perp}$	ε	K_d	D_a	$D_{a\square}$	$D_{a\perp}$	R	α	$\alpha_\square$	$\alpha_\perp$	
HTO	1.36E-11	2.40E-11	3.20E-12	0.16		8.50E-11	1.50E-10	2.00E-11					(Cormenzana et al., 2008)
HTO	3.44E-11	5.60E-11	1.28E-11	0.16		2.15E-10	3.50E-10	8.00E-11					(Cormenzana et al., 2008)
HTO	3.75E-11	6.00E-11	1.50E-11	0.15		2.50E-10	4.00E-10	1.00E-10					(Garcia-Gutierrez et al., 2006)
HTO	3.22E-11	5.00E-11	1.43E-11	0.15		2.14E-10							(Palut et al., 2003)
HTO	1.82E-11	3.10E-11	5.40E-12	1.45E-01		1.26E-10				1.45E-01	0.15	0.14	(Van Loon et al., 2004a)
HTO	1.87E-11	3.20E-11	5.40E-12	1.30E-01		1.44E-10				1.30E-01	0.13	0.13	(Van Loon et al., 2004a)
HTO	3.40E-11	5.40E-11	1.40E-11	1.60E-01		2.13E-10				1.60E-01	0.15	0.17	(Van Loon et al., 2004a)
HTO	3.40E-11	5.40E-11	1.40E-11	1.55E-01		2.19E-10				1.55E-01	0.17	0.14	(Van Loon et al., 2004a)
HTO	4.00E-11	4.00E-11		1.50E-01		2.67E-10				1.50E-01	0.15		(Van Loon et al., 2004a)
HTO	4.00E-11			0.15		2.67E-10							(Van Loon et al., 2004b)
HTO	6.00E-11			0.15		4.00E-10							(Wersin et al., 2008)
HTO	6.70E-12			0.15		4.47E-11							(Van Loon et al., 2003b)
HTO	5.90E-12			0.14		4.21E-11							(Van Loon et al., 2003b)
HTO	5.60E-12			0.13		4.31E-11							(Van Loon et al., 2003b)
HTO	1.50E-11			0.1		1.50E-10							(Van Loon et al., 2003a)
HTO	1.20E-11			0.1		1.20E-10							(Van Loon et al., 2003a)
D2O	2.50E-11	4.00E-11	1.00E-11	0.15									(Samper et al., 2006)
Cl	2.50E-12	4.00E-12	1.00E-12	8.06E-02		3.10E-11	5.00E-11	1.20E-11					(Garcia-Gutierrez et al., 2006)
Cl	9.10E-13			0.044									(Van Loon et al., 2003b)
Cl	7.90E-13			0.039									(Van Loon et al., 2003b)
Cl	7.10E-13			0.039									(Van Loon et al., 2003b)
Cl	5.70E-12			0.073									(Van Loon et al., 2003a)

Cl	4.10E-12			0.072									(Van Loon et al., 2003a)
Cl	2.04E-12	3.40E-12	6.70E-13	4.50E-02						4.50E-02	0.05	0.04	(Van Loon et al., 2004a)
Cl	1.01E-11	1.60E-11	4.10E-12	8.00E-02						8.00E-02	0.08	0.08	(Van Loon et al., 2004a)
Cl*	1.80E-11	1.80E-11		1.00E-01						1.00E-01	0.1		(van der Kamp and Van Stempvoort, 1998)
Cl*	5.60E-11	5.60E-11		1.50E-01						1.50E-01	0.15		(van der Kamp and Van Stempvoort, 1998)
I	5.17E-12	8.27E-12	2.07E-12	8.00E-02									(Samper et al., 2006)
I	6.60E-13			0.083									(Van Loon et al., 2003b)
I	5.00E-13			0.063									(Van Loon et al., 2003b)
I	4.50E-13			0.076									(Van Loon et al., 2003b)
I	4.80E-12			0.105									(Van Loon et al., 2003a)
I	3.40E-12			0.077									(Van Loon et al., 2003a)
I	1.00E-11	1.00E-11		0.09							0.09		(Van Loon et al., 2004a)
I	1.00E-11			0.085									(Van Loon et al., 2004b)
Br-*	1.70E-11	1.70E-11		0.1							0.1		(van der Kamp and Van Stempvoort, 1998)
Br-*	4.50E-11	4.50E-11		0.15							0.15		(van der Kamp and Van Stempvoort, 1998)
Na	4.55E-11					4.55E-11	7.80E-11	1.30E-11		1.00E+00	0.89	1.11	(Van Loon et al., 2004a)
Na	2.39E-11					4.35E-11	7.20E-11	1.50E-11		5.50E-01	0.62	0.48	(Van Loon et al., 2004a)
Na	3.84E-11					6.00E-11	6.00E-11			6.40E-01	0.64		(Van Loon et al., 2004a)
Na	6.00E-11									0.64			(Van Loon et al., 2004b)
Cs	1.35E-09					1.90E-13			1.92E+04	7.10E+03			(Maes et al., 2008)
Cs	4.05E-10					1.62E-13			6.80E+03	2.50E+03			(Maes et al., 2008)
Cs	1.10E-10					1.00E-13			2.90E+03	1.10E+03			(Maes et al., 2008)
Cs	2.00E-10								$s= 0.186c^{0.53}$				(Van Loon et al., 2004b)
Np(v)	6.90E-12			0.15	0.1					243			(Wu et al., 2009)

*the measured effective diffusion coefficient and accessible porosity are cited in Van Loon et al. (2004a).

Table 2. The minimum, maximum and average values for the effective diffusion coefficient D_e (m^2/s), accessible porosity ε, distribution coefficient K_d (mL/g), rock capacity factor α for Opalinus Clay.

Species	D_e			ε			α		
	min	**max**	**average**	**min**	**max**	**average**	**Min**	**max**	**average**
HTO	5.60E-12	6.00E-11	2.55E-11	0.100	0.160	0.143			
D2O			2.50E-11			0.150			
Cl	7.10E-13	1.01E-11	3.35E-12	0.039	0.081	0.059			
I	4.50E-13	1.00E-11	4.37E-12	0.063	0.105	0.082			
Br	1.70E-11	4.50E-11	3.10E-11	0.100	0.150	0.130			
Na	2.39E-11	6.00E-11	4.20E-11				0.55	1	0.708
Cs	1.10E-10	1.35E-09	5.16E-10				1100	7100	3570
Np(V)			6.90E-12						243

Table 3. Estimated data for the effective diffusion coefficients D_e (m^2/s), effective diffusion coefficients in directions parallel and perpendicular to the bedding of clay formation , $D_{e\square}$ (m^2/s) and $D_{e\perp}$ (m^2/s), accessible porosity ε, distribution coefficient K_d (mL/g), apparent diffusion coefficients in directions parallel to the bedding, $D_{a\perp}$ (m^2/s), and rock capacity factor α for Callovo-Oxfordian (COx) argillite.

Species	D_e	$D_{e\square}$	$D_{e\perp}$	ε	K_d	$D_{a\square}$	α	
HTO	1.1E-11			0.204			0.204	(Descostes et al., 2008)
HTO	4.4E-11			0.215			0.215	(Descostes et al., 2008)
HTO	3.3E-11			0.165			0.165	(Descostes et al., 2008)
HTO	4.7E-11			0.224			0.224	(Descostes et al., 2008)
HTO	4.9E-11			0.217			0.217	(Descostes et al., 2008)
HTO	1.4E-11			0.171			0.171	(Descostes et al., 2008)
HTO	2.5E-11			0.167			0.167	(Descostes et al., 2008)
HTO	2.7E-11			0.247			0.247	(Descostes et al., 2008)
HTO	1.88E-11	3.00E-11	7.50E-12	0.15				(Garcia-Gutierrez et al., 2008)
HTO	2.93E-11	4.50E-11	1.35E-11	0.15				(Garcia-Gutierrez et al., 2008)
HTO	1.78E-11			0.15				(Garcia-Gutierrez et al., 2008)
HTO	4.22E-11			0.15				(Garcia-Gutierrez et al., 2008)
HTO	3.75E-11			0.15				(Garcia-Gutierrez et al., 2008)
HTO	3.97E-11			0.15				(Garcia-Gutierrez et al., 2008)
HTO	4.10E-11			0.18				(Samper et al., 2008)
HTO	2.74E-11	4.04E-11	1.45E-11					(Samper et al., 2008)
HTO	3.06E-11	4.51E-11	1.61E-11					(Samper et al., 2008)
Cl	4.8E-13			0.049			0.049	(Descostes et al., 2008)
Cl	5.9E-12			0.064			0.064	(Descostes et al., 2008)
Cl	8.4E-12			0.077			0.077	(Descostes et al., 2008)
Cl	4.6E-12			0.065			0.065	(Descostes et al., 2008)

Cl	4.44E-12							(Garcia-Gutierrez et al., 2008)
Cl	8.86E-12							(Garcia-Gutierrez et al., 2008)
Cl	6.48E-12							(Garcia-Gutierrez et al., 2008)
Cl	8.01E-12							(Garcia-Gutierrez et al., 2008)
Cl	9.10E-12			0.09				(Samper et al., 2008)
I	2.3E-12			0.284			0.284	(Descostes et al., 2008)
I	4.7E-12			0.065			0.065	(Descostes et al., 2008)
I	4.6E-12			0.053			0.053	(Descostes et al., 2008)
I	1.6E-12			0.033			0.033	(Descostes et al., 2008)
I	4.40E-12			0.13				(Samper et al., 2008)
SeO_3^{2-}	1E-14			0.003			0.003	(Descostes et al., 2008)
SeO_3^{2-}	1.5E-13			0.009			0.009	(Descostes et al., 2008)
SO_4^{2-}	2.1E-13			0.107			0.107	(Descostes et al., 2008)
SO_4^{2-}	1.9E-12			0.307			0.307	(Descostes et al., 2008)
Na	2.75E-11			0.15	0.37			(Garcia-Gutierrez et al., 2008)
Na	6.09E-11			0.15	0.37			(Garcia-Gutierrez et al., 2008)
Na	6.70E-11			0.18	0.74			(Samper et al., 2008)
Sr	7.06E-12				0.87			(Garcia-Gutierrez et al., 2008)
Sr	2.63E-13			0.15	0.87	6.00E-13		(Garcia-Gutierrez et al., 2008)
Sr	8.77E-13			0.15	0.87	2.00E-12		(Garcia-Gutierrez et al., 2008)
Sr	2.70E-11	2.70E-11		0.16	1.09			(Samper et al., 2008)
Cs	3.60E-10			0.18	50			(Samper et al., 2008)

Table 4. The minimum, maximum and average values for effective diffusion coefficient D_e (m^2/s), accessible porosity ε, distribution coefficient K_d (ml/g) for COx argillite.

Species	D_e			ε			K_d		
	min	**max**	**average**	**min**	**max**	**Average**	**min**	**max**	**average**
HTO	1.10E-11	4.90E-11	3.14E-11	0.150	0.247	0.179			
Cl	4.80E-13	9.10E-12	6.25E-12	0.049	0.090	0.069			
I	1.60E-12	4.70E-12	3.52E-12	0.033	0.284	0.113			
SeO32-	1.00E-14	1.5E-13	8.00E-14	0.003	0.009	0.006			
SO42-	2.10E-13	1.90E-12	1.055E-12	0.107	0.307	0.207			
Na	2.75E-11	6.70E-11	5.18E-11	0.15	0.18	0.16	0.37	0.74	0.49
Sr	2.63E-13	2.70E-11	8.80E-12			0.15			0.87
Cs			3.60E-10			0.18			50

Table 5. Estimated values for effective diffusion coefficients D_e (m^2/s), accessible porosity ε, and distribution coefficient K_d (mL/g) for Toarcian clayey formation at the Tournemire experimental site (France).

Species	D_e	ε	K_d	
HTO	2.64E-11	0.124		(Motellier et al., 2007)

HTO	2.65E-11	0.124		(Motellier et al., 2007)
HTO	2.83E-11	0.124		(Motellier et al., 2007)
HTO	2.62E-11	0.124		(Motellier et al., 2007)
HTO	2.62E-11	0.124		(Motellier et al., 2007)
HTO	2.75E-11	0.124		(Motellier et al., 2007)
HTO	2.85E-11	0.124		(Motellier et al., 2007)
HTO	2.05E-11	0.124		(Motellier et al., 2007)
HTO	2.06E-11	0.124		(Motellier et al., 2007)
HTO	7.50E-12*	0.124		(Motellier et al., 2007)
HTO	7.9E-12*	0.124		(Motellier et al., 2007)
HTO	2.22E-11	0.124		(Motellier et al., 2007)
HTO	2.71E-11	0.124		(Motellier et al., 2007)
HTO	3.1E-11	0.124		(Motellier et al., 2007)
HTO	3.36E-11	0.124		(Motellier et al., 2007)
HTO	2.33E-11	0.124		(Motellier et al., 2007)
HTO	2.01E-11	0.124		(Motellier et al., 2007)
Cl	2.20E-12	0.02		(Savoye et al., 2006b)
Cl	3.80E-12	0.02		(Savoye et al., 2006b)
Cl	3.90E-12	0.03		(Savoye et al., 2006b)
Cl	2.60E-12	0.037		(Savoye et al., 2006b)
Cl	3.60E-12	0.037		(Savoye et al., 2006b)
Cl	4.20E-12	0.037		(Savoye et al., 2006b)
Cl	7.50E-12	0.038		(Savoye et al., 2006b)
Cl	4.10E-12	0.042		(Savoye et al., 2006b)
Cl	1.20E-12	0.02		(Patriarche et al., 2004b)
Cl	1.30E-12	0.021		(Patriarche et al., 2004b)
Cl	1.70E-12	0.02		(Patriarche et al., 2004b)
I	2.10E-12	0.037	0.00E+00	(Savoye et al., 2006b)
I	3.00E-12	0.037	0.00E+00	(Savoye et al., 2006b)
I	1.10E-11	0.12	3.50E-02	(Savoye et al., 2006b)
I	9.80E-12	0.14	3.50E-02	(Savoye et al., 2006b)
I	8.00E-12	0.16	5.50E-02	(Savoye et al., 2006b)
I	1.60E-11	0.2	6.40E-02	(Savoye et al., 2006b)
I	1.50E-11	0.21	6.70E-02	(Savoye et al., 2006b)
I	2.00E-11	0.25	8.20E-02	(Savoye et al., 2006b)
Br	2.00E-12	0.042		(Savoye et al., 2006b)
Br	3.10E-12	0.05		(Savoye et al., 2006b)
Br	3.40E-12	0.048		(Savoye et al., 2006b)
Br	3.40E-12	0.038		(Savoye et al., 2006b)

* measured in an orientation 90° to horizontal

Table 6. The minimum, maximum and average values for the effective diffusion coefficient D_e (m^2/s), accessible porosity ε, distribution coefficient K_d (mL/g) for Toarcian clayey formation at the Tournemire experimental site (France).

Species	D_e			ε			K_d		
	min	max	ave	min	max	ave	min	max	ave
HTO	7.50E-12	3.36E-11	2.37E-11			0.124			
Cl	1.20E-12	7.50E-12	3.28E-12	0.020	0.042	0.029			
I	2.10E-12	2.00E-11	1.06E-11	3.70E-02	2.50E-01	1.44E-01	0.00E+00	2.50E-01	4.23E-02
Br	2.00E-12	3.40E-12	2.98E-12						

Table 7. Values for effective diffusion coefficient (m^2/s) of different species for Opalinus Clay (OPc), Callovo-Oxfordian (COx) argillite and Toarcian clayey formations (TOc) .

Clay rock	**HTO**		**Cl**		**I**		**Br**		**Na**		**Cs**	
	Max /min	**Average**	**Max /min**	**Average**	**Max /min**	**Average**	**Max /min**	**Average**	**Max /min**	**Average**	**Max /min**	**Average**
OPc	10.7	2.55E-11	14.2	3.35E-12	22.2	4.37E-12	2.69	3.1E-11	2.5	4.2E-11	12.2	5.16E-10
COx	4.4	3.14E-11	18.92	6.25E-12	2.9	3.52E-12			2.4	5.18E-11		3.6E-10
TOc	4.5	2.37E-11	6.3	3.28E-12	9.5	1.06E-11	9.5	2.98E-12				

Table 8. Values for accessible porosity of different species for Opalinus Clay (OPc), Callovo-Oxfordian (COx) argillite, and Toarcian clayey formations (TOc) .

Clay rock	**HTO**		**Cl**		**I**	
	Max/min	**Average**	**Max/min**	**Average**	**Max/min**	**Average**
OPc	1.6	0.14	2.1	0.059	1.7	0.082
COx	1.6	0.18	1.8	0.069	3.9	0.070
TOc		0.12	2.1	0.029	6.8	0.144

3. AN IMPROVED MODELING APPROACH

Because of its computational and conceptual simplicity, the phenomenological approach has often been used for analyzing diffusion experiment results (Section 2.2) and also seems to be a natural choice for system-level modeling of diffusion processes. However, as previously indicated, this approach is subject to a number of limitations, mainly because it does not account for the effects of detailed electrochemical processes. This section presents an improved modeling approach to remove some of these limitations. In particular, our model development focuses on two questions that are fundamental to modeling diffusion processes in natural clay rock (within the context of system-level modeling): (1) Can Fick's law be an acceptable approximation for modeling diffusion? (2) How can essential features of electrochemical processes be incorporated into a simple diffusion model? As discussed later, answers to these questions may be different for dense clay (bentonite) and natural clay rock: our focus here is on the latter.

3.1 Theoretical Basis

For simplicity, we divide pore water into two parts: (1) mobile water in macropores that is not subject to electrochemical processes, and (2) pore water with DDL (including interlayers) that is strongly impacted

by electrochemical processes. Based on the Donnan approximation, the electrochemical potential of species *i* is given by (Appelo et al. 2010):

$$\mu_{i,D} = \mu_i^0 + RT\ln a_{i,D} + z_i F\varphi \tag{8}$$

where subscript *D* refers to average properties within DDL, μ_i^0 is the standard potential, *R* is the gas constant, *T* is the absolute temperature, $a_{i,D}$ is the activity, z_i is the charge number, *F* is Faraday constant, and φ is the electrical potential.

The chemical potential for macropore water, μ_i , is described by

$$\mu_i = \mu_i^0 + RT\ln a_i \tag{9}$$

where a_i is the activity for the macropore water. It is commonly assumed that at local scale, chemical equilibrium exists (e.g., Appelo et al. 2010; Leroy et al. 2007), or chemical potentials defined in Equations (8) and (9) are equal. Therefore, we have from Equations (8) and (9)

$$a_{i,D} = a_i exp\left\{-\frac{z_i\varphi}{RT}\right\} \tag{10}$$

Based on the general relationship between diffusion flux and gradient of chemical potential (Appelo et al. 2010; Leroy et al. 2007), and considering that the total diffusion flux is the summation of fluxes for macropore water and the DDL, we obtain the total flux:

$$J_i = -f\frac{D_{e,M}C_i}{RT}\nabla\mu_i - \frac{(1-f)(D_{e,D}C_{i,D})}{RT}\nabla\mu_{i,D} \tag{11}$$

where *f* is the volumetric fraction of macopore water in the pore porosity, and *C* is concentration. $D_{e,M}$ and $D_{e,D}$ are effective diffusion coefficients for macropore space and the DDL, respectively, and can be calculated following Eq. (3). Considering the practical difficulty in determining tortuosity and constrictivity independently for both macropore water and the DDL, we assume here that they are the same as the first order of approximation. In this case, we can derive from Equation (3):

$$D_{e,M} - D_{e,D} - \frac{D_{e,HTO}D_{w,i}}{D_{w,HTO}} \tag{12}$$

where subscript *w* refers to the diffusion coefficient in free water, and $D_{e,HTO}$ is the effective diffusion coefficient (defined by Equation (3)) for HTO that is not subject to electrochemical processes.

If we further assume the reactivity coefficient (the ratio of activity to concentration) to be one for both parts of pore water, we obtain the following relationship between diffusive flux and concentration gradient by combining Equations (9), (10), and (11):

$$J_i = -D_{e,M}\left\{f + (1-f)exp\left[-\frac{z_i\varphi}{RT}\right]\right\}\nabla C_i \tag{13}$$

The derivation of Equation (13) employs a previously discussed approximation that at local scale, chemical potentials are the same for the DDL and macropore water. One important implication from Equations (13) is that Fick's law is still applicable for modeling the diffusion process in natural clay, largely resulting from the fact that macropore water (that is not subject to electro-mechanical process)

exists, such that the chemical potential gradient in the two parts of the water can be described by the concentration gradient corresponding to the macropore–water part. This may not be the case for EBS bentonite, in which DDL overlapping may occur, even within a relatively large pore (Steefel et al. 2010).

From (13), the effective diffusion coefficient can be written as

$$D_{e,i} = D_{e,M}\left\{f + (1-f)exp\left[-\frac{z_i\varphi}{RT}\right]\right\} \tag{14}$$

Note that in the above equation, the electrical potential may change with the reactive transport process (such as a change in ionic strength). For a natural clay formation, the electrical potential may not change significantly (Jougnot et al. 2009). Therefore, in this study, we assume that potential to be constant.

It is of interest to compare our approach with the commonly used phenomenological approach (Section 2.1.1). Both approaches calculate diffusion flux using Fick's law, and consequently our approach has a computational efficiency similar to that of the phenomenological approach. However, our approach explicitly considers the effects of electrochemical processes, although we employed a number of assumptions/approximations, based on the practical consideration that model simplicity is a desirable feature for system-level models.

3.2 Preliminary Evaluation

In Section 3.1, we proposed an improved diffusion model that considers the effects of electrochemical processes through the dependence of an effective diffusion coefficient on electrical properties of clay rock (Equation (14)). In other words, the key element of our approach is Equation (14), which can be rearranged as

$$\frac{D_{e,i}}{D_{e,M}} = f + (1-f)exp\left[-\frac{z_i\varphi}{RT}\right] \tag{15}$$

Therefore, the evaluation of the approach focuses on examining how Equation (15) represents parameter values obtained from experimental observations.

Figure 4 shows a comparison between measured and calculated values for the ratio of diffusion coefficient ($\frac{D_{e,i}}{D_{e,M}}$). The filled and open rectangles in the figure correspond to data points for Opalinus Clay from Appelo et al. (2010) and Wersin et al. (2008), respectively. These data points represent results for HTO, Cl^-, B_r^-, I^-, Cs^+, N_a^+, $^{85}Sr^{2+}$ and $^{60}Co^{2+}$. To calculate diffusion-coefficient ratio from the data, we calculate $D_{e,M}$ from Equation (12) with water self-diffusion coefficient, and diffusion coefficient in free water, for a corresponding chemical species determined from Harris and Woolf (1980) and Li and Gregory (1974), respectively.

To calculate the diffusion coefficient ratio using Equation (15), we treat f and $A = \frac{\varphi}{RT}$ as two fitting factors in this study. (While they may be able to be determined independently from relevant data, an acceptable approach for doing so is not yet available in the literature.) The solid curve in the figure is the best match of Equation (15) to the data for a given $f = 0.4$. The parameter f was not further adjusted to optimize the match. The dashed line corresponds to the same A value as the solid line, but a different f value (0.2). Differences between these two curves are not considered significant, indicating that the ratio calculated from Equation (15) is not very sensitive to f within a certain range of f values. The comparison

between calculated and observed results is fairly reasonable, supporting the usefulness of our approach. However, notable differences between observed and calculated ratio values occur for C_S^+ (the three data points with ratio values larger than 3 for $z_i = 1$ in Figure 4). Note that for highly adsorbed cations like C_S^+, as previously discussed, measured concentration or flux data used to determine diffusion coefficient estimates are not very sensitive to values for the diffusion coefficient, so that the corresponding estimates (or data points in Figure 4) might have rather large uncertainty. Also, Figure 4 only includes a few data points for Opalinus Clay; we are planning to use all the data presented in Section 2.2 to further evaluate the approach in the future.

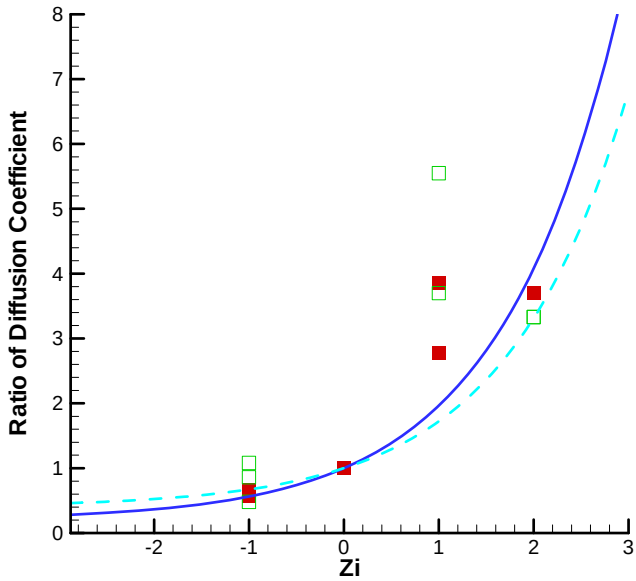

Figure 4. Comparison between calculated (curves) and observed (rectangles) values for ratio of diffusion coefficient as a function of charge number z_i.

To further examine the practical usefulness of incorporating the effects of electrochemical effects into an effective diffusion coefficient, we check whether observed breakthrough curves can be captured by a modeling approach based on Fick's law and treating diffusion coefficient as an uncertain parameter. (The uncertainty partially comes from the treatment of electrochemistry effects.) This is highly relevant to system-level models for diffusion in clay, because they use Fick's law and allow for consideration of parameter uncertainty. We evaluate this issue with results from an *in situ* diffusion test using inert and reactive tracers (DIR) at the Bure site in France (Samper et al. 2008).

ANDRA has undertaken an extensive characterization program at the Bure site to assess the feasibility of a deep high-level radioactive waste (HLW) repository in the Callovo–Oxfordian (COx) clay. Diffusion of inert and reactive tracers (DIR) is one of several experimental programs that aim at characterizing diffusion and retention of radionuclides in clay rock. Figure 5 shows the sketch of the experiment. The experiment was an *in situ* single-point dilution test that involved injecting tracers into a 1 m long packed-off section of the boreholes. Details of the experiment are given in Samper et al. (2008).

The conventional approach requires calibrating the accessible porosity and effective diffusion coefficient for anions. For this study based on the proposed approach, we use total porosity and the effective diffusion coefficient from Equation (15). In this report, we use the same numerical model as developed in Samper et al. (2008). The model uses 2D axi-symmetric finite element mesh and the simulation is

conducted with INVERSE-CORE^{2D} (Dai and Samper 2004). Figure 6 shows the measured chloride concentration, the optimal accessible porosity, and the effective diffusion coefficient. Also shown in Figure 6 is the model results with total porosity (0.18) and several possible effective diffusion coefficients calculated from Equation (15). It shows that our approach leads to either very similar results to the reference model, or results within the error of measured data.

Our approach considers the DDL effect by modifying the effective diffusion coefficient but not the adsorption. In other words, the distribution coefficient or retardation factor is still needed when applying our approach. Those model results, shown in Figure 7, have a distribution coefficient of 1.13 ml/g. We also model the diffusion of sodium (Figure 7) with two other effective diffusion coefficients: 3.4e-11 m^2/s, which is about 2/3 of the reference value, and 8.5e-12 m^2/s, which is about 1/6 of the reference value. Compared with the reference model, the model with smaller diffusion coefficient deviates from the best fit, but the effect is rather minimal.

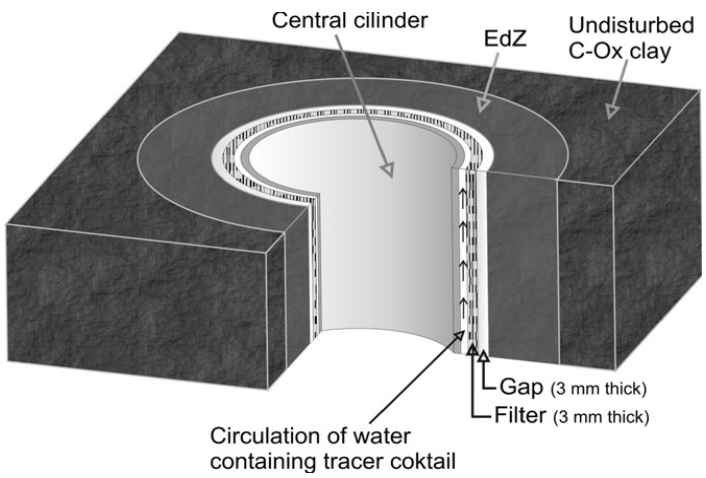

Figure 5. Sketch of borehole geometry for DIR experiments (Samper et al. 2008)

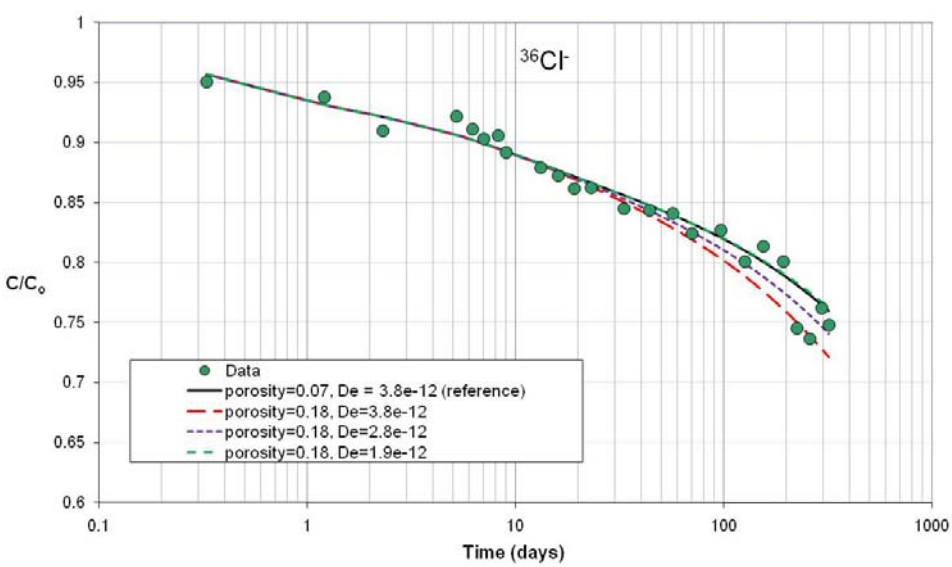

Figure 6. Measured (Samper et al. 2008) and computed Cl concentration with several effective diffusion coefficients (m^2/s).

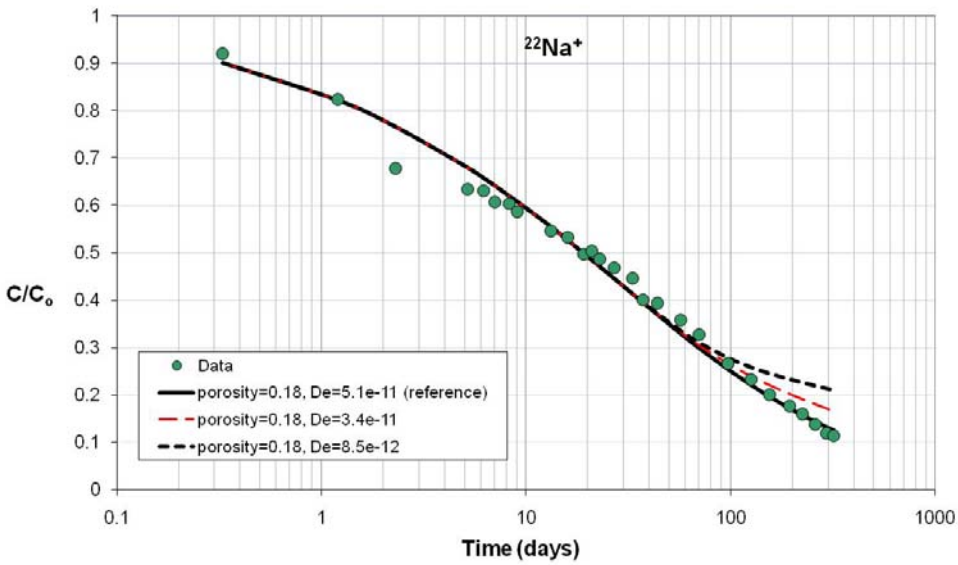

Figure 7. Measured (Samper et al. 2008) and computed Na concentration with several effective diffusion coefficients (m^2/s).

4. CONCLUDING REMARKS

Summary

Diffusion is the dominant mechanism for radionuclide transport in a clay repository. Modeling of diffusive transport in clay rocks is complicated by the existence of heterogeneity at different scales and coupling between diffusive and electro-chemical processes. This report reviews the two kinds of modeling approaches. Phenomenological approaches are based on Fick's diffusion law and use semi-empirical constants to roughly incorporate the effects of electro-chemical processes. While they cannot capture the detailed transport mechanisms and therefore inherently introduce a certain modeling uncertainty, they relatively simple, computationally efficient, and straightforward to implement. Mechanistic approaches are based on detailed and explicit descriptions of interaction between diffusion processes and electro-chemical processes. They do not suffer the limitations of phenomenological approaches, but are computationally more complex and involve more parameters. This report also reviews and compiles data sets of parameters related to diffusive transport in clay formations that are available in the literature. These data sets provide useful information for evaluating modeling approaches and can be used as inputs into relevant models. An improved modeling approach is proposed to combine the advantages of phenomenological and mechanistic approaches. Results from a preliminary evaluation of the approach are encouraging.

Future Work

- Continue to evaluate the proposed modeling approach with more data. The approach has been evaluated with a few data points (Figure 4) and by a comparison between simulation results based on the approach and test observations. More evaluations are needed to improve and/or increase the confidence in the approach.
- Investigate the impact of heterogeneity (and anisotropy) on large-scale diffusion process by comparing simulation results with apparent diffusion coefficients and without considering

heterogeneity and those theoretical and numerical results that explicitly consider heterogeneity. The outcome should be useful for determining how the heterogeneity should be treated in system-level modeling of diffusion in clay.

- Integrate process modeling of diffusion in clay with system-level modeling. LBNL will work with ANL to develop process-modeling results to support ANL's system-level diffusion model for clay.
- Study the impact of electrochemical process on large-scale diffusion. As previously indicated, our knowledge of this impact is still lacking. Once a rigorous mechanistic approach is available from the EBS work (e.g., Steefel et al. 2010), we will compare simulation results obtained with our proposed and the mechanistic approaches for a large-scale problem to check how well our approach can capture the large-scale electro-chemical process.

Reference

Aertsens, M., P. De Canniere, K. Lemmens, N. Maes and H. Moors 2008. *Overview and consistency of migration experiments in clay*. Physics and Chemistry of the Earth 33(14-16): 1019-1025.

Appelo, C. A. J., L. R. Van Loon and P. Wersin 2010. *Multicomponent diffusion of a suite of tracers (HTO, Cl, Br, I, Na, Sr, Cs) in a single sample of Opalinus Clay*. Geochimica et Cosmochimica Acta 74(4): 1201-1219.

Appelo, C. A. J., A. Vinsot, S. Mettler and S. Wechner 2008. *Obtaining the porewater composition of a clay rock by modeling the in- and out-diffusion of anions and cations from an in-situ experiment*. Journal of Contaminant Hydrology 101(1-4): 67-76.

Appelo, C. A. J. and P. Wersin 2007. *Multicomponent Diffusion Modeling in Clay Systems with Application to the Diffusion of Tritium, Iodide, and Sodium in Opalinus Clay*. Environmental Science & Technology 41(14): 5002-5007.

Barenblatt, G. I. and I. P. Zheltov 1960. *Fundamental Equations for the Filtration of Homogeneous Fluids through Fissured Rocks*. Doklady Akademii Nauk Sssr 132(3): 545-548.

Barnichon J.D., and G. Volckaert 2003. *Observations and Predictions of Hydromechanical Coupling Effects in the Boom Clay, Mol Underground Research Laboratory, Belgium*, Hydrogeology Journal 11 (1), 193-202.

Bourg, I. C., A. C. M. Bourg and G. Sposito 2003. *Modeling diffusion and adsorption in compacted bentonite: a critical review*. Journal of Contaminant Hydrology 61(1-4): 293-302.

Cormenzana, J., M. Garcia-Gutierrez, T. Missana and U. Alonso 2008. *Modelling large-scale laboratory HTO and strontium diffusion experiments in Mont Terri and Bure clay rocks*. Physics and Chemistry of the Earth 33(14-16): 949-956.

Dai, Z., J. Samper 2004. *Inverse problem of multicomponent reactive chemical transport in porous media: formulation and applications*. Water Resour. Res. 40, W07407. doi:10.1029/2004WR00324.

Descostes, M., V. Blin, F. Bazer-Bachi, P. Meier, B. Grenut, J. Radwan, M. L. Schlegel, S. Buschaert, D. Coelho and E. Tevissen 2008. *Diffusion of anionic species in Callovo-Oxfordian argillites and Oxfordian limestones (Meuse/Haute-Marne, France)*. Applied Geochemistry 23(4): 655-677.

ENRESA 2000. *Full-scale engineered barriers experiment for a deep geological repository in crystalline host rock FEBEX Project*, European Commission**:** 403.

Fouche O., H. Wright, J. L. Cleach, and P. Pellenard 2004. *Fabric Control on Strain and Rupture of Heterogeneous Shale Samples by Using a Non-Conventional Mechanical Test*. Applied Clay Science 26, 367-387.

Gonzales S., and K. S. Johnson 1984. *Shale and other argillaceous strata in the United States*. Oak Ridge National Laboratory. ORNL/Sub/84-64794/1.

Garcia-Gutierrez, M., J. L. Cormenzana, T. Missana, M. Mingarro, U. Alonso, J. Samper, Q. Yang and S. Yi 2008. *Diffusion experiments in Callovo-Oxfordian clay from the Meuse/Haute-Marne URL, France. Experimental setup and data analyses*. Physics and Chemistry of the Earth 33: S125-S130.

Garcia-Gutierrez, M., J. L. Cormenzana, T. Missana, M. Mingarro and P. L. Martin 2006. *Large-scale laboratory diffusion experiments in clay rocks*. Physics and Chemistry of the Earth 31(10-14): 523-530.

Gerke, H. H. and M. T. van Genuchten 1993a. *A dual porosity model for simulating the preferential movement of water and solutes in structured porous media*. Water Resour. Res. 29: 305-319.

Gerke, H. H. and M. T. van Genuchten 1993b. *Evaluation of a first order water transfer term for variably saturated dual porosity flow models.* Water Resour. Res. 29: 1225-1238.

Gerke, H. H. and M. T. van Genuchten 1996. *Macroscopic representation of structural geometry of simulating water and solute movement in dual-porosity media*. Adv. Water Resour. 19: 343-357.

Hantush, M. M., R. S. Govindaraju, M. A. Mariño and Z. Zhang 2002. *Screening model for volatile pollutants in dual porosity soils*. J. Hydrol. 260: 58-74.

Hantush, M. M., M. A. Mariño and M. R. Islam 2000. *Models for leaching of pesticides in soils and groundwater*. J. Hydrol. 227: 66-83.

Harris, K.R., and L. A. Woolf 1980. *Pressure and Temperature Dependence of the Self Diffusion Coefficient of Water and Oxygen-18 Water*. J.C.S. Faraday I 76: 377-385.

Jougnot, D., A. Revil and P. Leroy 2009. *Diffusion of ionic tracers in the Callovo-Oxfordian clay-rock using the Donnan equilibrium model and the formation factor*. Geochimica et Cosmochimica Acta 73(10): 2712-2726.

Leroy, P., A. Revil, S. Altmann, and C. Tournassat 2007. *Modeling the Composition of the Pore Water in a Clay-Rock Geological Formation (Callovo-Oxfordian, France).* Geochimica et Cosmochimica Acta 71: 1087-1097.

Li, Y.H., and S. Gregory 1974. *Diffusion of Ions in Sea Water and in Deep-Sea Sediments.* Geochimica et Cosmochimica Acta 38: 703-714.

Lichtner, P. C. 2000. *Critique of dual continuum formulation of multicomponent reactive transport in fractured porous media.* Geophysical Monograph 122: 281-298.

Maes, N., S. Salah, D. Jacques, M. Aertsens, M. Van Gompel, P. De Cannière and N. Velitchkova 2008. *Retention of Cs in Boom Clay: Comparison of data from batch sorption tests and diffusion experiments on intact clay cores*. Physics and Chemistry of the Earth, Parts A/B/C 33(Supplement 1): S149-S155.

Meier P., T. Trick, P. Blumling, and G. Volckaert 2000. *Self-Healing of Fractures within the EDZ at the Mont Terri Rock Laboratory: Results after One Year of Experimental Work*. In: Proceedings of the International Workshop on Geomechanics, hydromechanical and Thermomechanical Behavior of Deep Argillaceous Rocks: Theory and Experiments, Paris, October11-12, 2000.

Nutt M. 2011. *Used Fuel Disposition Campaign Disposal Research and Development Roadmap* (FCR&D-USED-2011-000065 REV0), U.S. DOE Used Fuel Disposition Campaign.

Motellier, S., I. Devol-Brown, S. Savoye, D. Thoby and J. C. Alberto 2007. *Evaluation of tritiated water diffusion through the Toarcian clayey formation of the Tournemire experimental site (France)*. Journal of Contaminant Hydrology 94(1-2): 99-108.

Palut, J. M., P. Montarnal, A. Gautschi, E. Tevissen and E. Mouche 2003. *Characterisation of HTO diffusion properties by an in situ tracer experiment in Opalinus clay at Mont Terri*. Journal of Contaminant Hydrology 61(1-4): 203-218.

Patriarche D., E. Ledoux , R. Simon-Coincon, J. Michelot, and J. Cabrera 2004a. *Characterization and Modeling of Diffusive Process for Mass Transport through the Tournemire Argillites Aveyron, France*. Applied Clay Science 26: 109-122.

Patriarche, D., J.-L. Michelot, E. Ledoux and S. Savoye 2004b. *Diffusion as the main process for mass transport in very low water content argillites: 1. Chloride as a natural tracer for mass transport;Diffusion coefficient and concentration measurements in interstitial water*. Water Resour. Res. 40(1): W01516.

Pruess, K. and T. N. Narasimhan 1985. *A practical method for modeling fluid and heat flow in fractured porous media*. Soc.Pet.Eng. J. 25: 14-26.

Ray, C., T. R. Ellsworth, A. J. Valocchi and C. W. Boast 1997. *An improved dual porosity model for chemical transport in macroporous soils.* J. Hydrol. 162: 279-298.

Revil, A. and P. Leroy 2004. *Constitutive equations for ionic transport in porous shales*. JOURNAL OF GEOPHYSICAL RESEARCH 109: B03208.

Samper, J., S. Dewonck, L. Zheng, Q. Yang and A. Naves 2008. *Normalized sensitivities and parameter identifiability of in situ diffusion experiments on Callovo-Oxfordian clay at Bure site*. Physics and Chemistry of the Earth, Parts A/B/C 33(14-16): 1000-1008.

Samper, J., C. Yang, A. Naves, A. Yllera, A. Hernández, J. Molinero, J. M. Soler, P. Hernán, J. C. Mayor and J. Astudillo 2006. *A fully 3-D anisotropic numerical model of the DI-B in situ diffusion experiment in the Opalinus clay formation*. Physics and Chemistry of the Earth, Parts A/B/C 31(10-14): 531-540.

Samper, J., Q. Yang, S. Yi, M. Garcia-Gutierrez, T. Missana, M. Mingarro, U. Alonso and J. L. Cormenzana 2008. *Numerical modeling of large-scale solid-source diffusion experiments in Callovo-Oxfordian clay*. Physics and Chemistry of the Earth 33: S208-S215.

Samper, J., L. Zheng, A. M. Fernández and L. Montenegro 2008. *Inverse modeling of multicomponent reactive transport through single and dual porosity media*. Journal of Contaminant Hydrology 98(3-4): 115-127.

Savoye, S., J. L. Michelot and C. Wittebroodt 2006a. *Evaluation of the reversibility of iodide uptake by argillaceous rocks by the radial diffusion method*. Radiochimica Acta 94(9-11): 699-704.

Savoye, S., J. L. Michelot, C. Wittebroodt and M. V. Altinier 2006b. *Contribution of the diffusive exchange method to the characterization of pore-water in consolidated argillaceous rocks*. Journal of Contaminant Hydrology 86(1-2): 87-104.

Šimunek, J., N. J. Jarvis, M. T. Van Genuchten and A. Gärdenäs 2003. *Review and comparison of models for describing non-equilibrium and preferential flow and transport in the vadose zone.* J. Hydrol. 272: 14-35.

Steefel C., J. Rutqvist, C.F. Tsang, H. H. Liu, E. Sonnenthal, J. Houseworth, and J. Birkholzer 2010. *Reactive Transport and Coupled THM Processes in Engineered Barrier System (EBS).* Lawrence Berkeley National Laboratory. LBNL Report LBNL-3901E.

Thury, M. 2002. *The characteristics of the Opalinus Clay investigated in the Mont Terri underground rock laboratory in Switzerland*. Comptes Rendus Physique 3(7-8): 923-933.

Van der Kamp, G., D. R. Van Stempvoort 1998. *Water sampling (laboratory) experiment (WS-B). Laboratory measurement of porosity, pore water isotopic composition and effective diffusivities of Opalinus Clay core samples*. Mont Terri Project, Technical Note 99-38, 1998.

Van Loon, L. R., J. M. Soler and M. H. Bradbury 2003a. *Diffusion of HTO, 36Cl- and 125I- in Opalinus Clay samples from Mont Terri: Effect of confining pressure*. Journal of Contaminant Hydrology 61(1-4): 73-83.

Van Loon, L. R., J. M. Soler, A. Jakob and M. H. Bradbury 2003b. *Effect of confining pressure on the diffusion of HTO, Cl-36(-) and I-125(-) in a layered argillaceous rock (Opalinus Clay): diffusion perpendicular to the fabric*. Applied Geochemistry 18(10): 1653-1662.

Van Loon, L. R., J. M. Soler, W. Müller and M. H. Bradbury 2004a. *Anisotropic Diffusion in Layered Argillaceous Rocks: A Case Study with Opalinus Clay*. Environmental Science & Technology 38(21): 5721-5728.

Van Loon, L. R., P. Wersin, J. M. Soler, J. Eikenberg, T. Gimmi, P. Hernan, S. Dewonck and S. Savoye 2004b. *In-situ diffusion of HTO, $^{22}Na^{+}$, Cs^{+} and I^{-} in Opalinus clay at the Mont Terri underground rock laboratory*. Radiochim. Acta 92: 757-763.

Van Loon, L.R., and A. Jacob 2005. *Evidence for a Second Transport Porosity for the Diffusion of Tritiated Water (HTO) in a Sedimentary Rock (Opalinus Clay –OPA): Application of Through- and Out-Diffusion Techniques*. Transport in Porous Media, 61:193-214.

Wersin, P., J. M. Soler, L. Van Loon, J. Eikenberg, B. Baeyens, D. Grolimund, T. Gimmi and S. Dewonck 2008. *Diffusion of HTO, Br-, I-, Cs+, 85Sr2+ and 60Co2+ in a clay formation: Results and modelling from an in situ experiment in Opalinus Clay*. Applied Geochemistry 23(4): 678-691.

Wilson, G. V., P. M. Jardine and J. P. Gwo 1992. *Modeling the hydraulic properties of a multiregion soil.* Soil Sci. Soc. Am. J. 56: 1731-1737.

Wu, T., S. Amayri, J. Drebert, L. R. Van Loon and T. Reich 2009. *Neptunium(V) Sorption and Diffusion in Opalinus Clay*. Environmental Science & Technology 43(17): 6567-6571.

Zheng L, J. Samper 2011. *Dual continuum multicomponent reactive transport with n-th order solute transfer terms for structured unsaturated porous media*. Water Resources Research, In review.